STRAIN AND TEMPERATURE CHANGES DURING THE POLYMERIZATION OF AUTOPOLYMERIZING ACRYLIC RESINS

Hyung-Jun Ahn, D.D.S., M.S.D., Chang-Whe Kim D.D.S., M.S.D., Ph.D., Yung-Soo Kim, D.D.S., M.S.D., Ph.D.
Department of Prosthodontics, Graduate School of Dentistry, Seoul National University

The aims of this experiment were to investigate the strain and temperature changes simultaneously within autopolymerzing acrylic resin specimens. A computerized data acquisition system with an electrical resistance strain gauge and a thermocouple was used over time periods up to 180 minutes. The overall strain kinetics, the effects of stress relaxation and additional heat supply during the polymerization were evaluated.

Stone mold replicas with an inner butt-joint rectangular cavity (40.0 x 25.0mm, 5.0mm in depth) were duplicated from a brass master mold. A strain gauge (AE-11-S50N-120-EC, CAS Inc., Korea) and a thermocouple were installed within the cavity, which had been connected to a personal computer and a precision signal conditioning amplifier (DA1600 Dynamic Strain Amplifier, CAS Inc., Korea) so that real-time recordings of both polymerization-induced strain and temperature changes were performed. After each of fresh resin mixture was poured into the mold replica, data recording was done up to 180 minutes with three-second interval. Each of two poly(methyl methacrylate) products (Duralay, Vertex) and a vinyl ethyl methacrylate product (Snap) was examined repeatedly ten times. Additionally, removal procedures were done after 15, 30 and 60 minutes from the start of mixing to evaluate the effect of stress relaxation after deflasking. Six specimens for each of nine conditions were examined. After removal from the mold, the specimen continued bench-curing up to 180 minutes. Using a waterbath (Hanau Junior Curing Unit, Model No.76-0, Teledyne Hanau, New York, U.S.A.) with its temperature control maintained at 50℃, heat-soaking procedures with two different durations (15 and 45 minutes) were done to evaluate the effect of additional heat supply on the strain and temperature changes within the specimen during the polymerization. Five specimens for each of six conditions were examined.

Within the parameters of this study the following results were drawn :

1. The mean shrinkage strains reached -3095$\mu\varepsilon$, -1796$\mu\varepsilon$ and -2959$\mu\varepsilon$ for Duralay, Snap and Vertex, respectively. The mean maximum temperature rise reached 56.7℃, 41.3℃ and 56.1℃ for Duralay, Snap, and Vertex, respectively. A vinyl ethyl methacrylate product (Snap) showed significantly less polymerization shrinkage strain ($p<0.01$) and significantly lower maximum temperature rise ($p<0.01$) than the other two poly(methyl methacrylate) products (Duralay, Vertex).
2. Mean maximum shrinkage rate for each resin was calculated to -31.8$\mu\varepsilon$/sec, -15.9$\mu\varepsilon$/sec and -31.8 $\mu\varepsilon$/sec for Duralay, Snap and Vertex, respectively. Snap showed significantly lower maximum shrinkage rate than Duralay and Vertex ($p<0.01$).

3. From the second experiment, some expansion was observed immediately after removal of specimen from the mold, and the amount of expansion increased as the removal time was delayed. For each removal time, Snap showed significantly less strain changes than the other two poly(methyl methacrylate) products ($p<0.05$).
4. During the external heat supply for the resins, higher maximum temperature rises were found. Meanwhile, the maximum shrinkage rates were not different from those of room temperature polymerizations.
5. From the third experiment, the external heat supply for the resins during polymerization could temporarily decrease or even reverse shrinkage strains of each material. But, shrinkage re-occurred in the linear nature after completion of heat supply.
6. Linear thermal expansion coefficients obtained from the end of heat supply continuing for an additional 5 minutes, showed that Snap exhibited significantly lower values than the other two poly(methyl methacrylate) products ($p<0.01$). Moreover, little difference was found between the mean linear thermal expansion coefficients obtained from two different heating durations ($p>0.05$).

Key Words
Acrylic resins, Polymerization shrinkage, Strain gauge

Autopolymerizing acrylic resins have been widely used in numerous clinical and laboratory procedures in dentistry for many purposes ranging from denture bases to inlay patterns. They have been generally advocated for direct post and core patterns,[1,2] soldering indexes for fixed partial dentures,[3,4] and provisional restorations. Generally, they have reasonable properties during manipulation[5] and their speed of polymerization is compatible with direct intraoral use. Relatively low cost, good reproduction of detail, and the fact that no additional equipment is required for curing are also attractive features. Meanwhile, their polymerization shrinkage and excessive heat release involved in the use of these resins are still challenging problems.

Autopolymerizing acrylic resins have their inherent property of polymerization shrinkage.[6] The conversion of monomer molecules into a polymer network is accompanied by comparable volumetric contraction,[7] which leads to inevitable dimensional changes. For many clinical situations, these dimensional changes do not cause any detrimental effects to the final outcome of overall prosthodontic treatment; however, serious and time-consuming problems can take place. The problems can be attributed to the resin' s dimensional inaccuracy, especially in case of numerous precision-demanding clinical procedures such as long-span provisonal restorations, and soldering procedure for multiunit fixed partial dentures.

Several measurement methods have been developed and advocated for evaluating polymerization shrinkage of various types of resinous materials.[8] Broadly, these methods can be divided into two categories : the volumetric shrinkage measurement methods and the linear shrinkage measurement methods. In the latter category, strain gauge method has several advantages. The post-gel shrinkage,[9-12] which is regarded as the major part of overall linear shrinkage can be monitored easily and accurately. The performance characteristics of strain gauges apply equally well to positive and negative linear change in general. Moreover, real-time measurement

is fully achieved with adequate hardware and software set-up so that time-dependent analysis of the polymerization shrinkage can be easily accomplished.

Recently, Kawara et al.[13] reported on the polymerization shrinkage kinetics of heat-activated acrylic denture base resins, using the strain gauge method. It was ascertained that the shrinkage of heat-activated acrylic denture base resins seems to mainly depend on thermal shrinkage phenomenon. Komiyama et al.[14] also investigated a residual stress relaxation in heat-activated acrylic denture bases fabricated by conventional polymer-monomer mixture method. It was revealed that a great deal of strain changes occurred during the deflasking procedure and their magnitudes depended on the lapse of time after completion of coolling. Currently there have been few reports dealing with analyzing time-based strain changes during the polymerization process of autopolymerizing acrylic resins using the strain gauge method.

This study consists of three successive experiments. The purpose of the first experiment was obtaining basic strain and temperature profiles of autopolymerizing acrylic resins. The second experiment aimed at verifying the effects of the removal procedure equivalent to the deflasking procedure in conventional denture processing on the strain profiles in the first experiment. The final experiment was performed to find out the effects of an external heat supply on the basic strain and temperature profiles in order to evaluate the thermal contraction as one of the major contributing factors for polymerization shrinkage of autopolymerizing acrylic resins.

MATERIALS AND METHODS

Materials

Details of the three autopolymerizing acrylic resins are shown in Table Ⅰ. For Duralay and Vertex, the powder consists of poly(methyl methacrylate) and initiator and the liquid contains monomer and activator. For Snap, the powder mainly consists of vinyl ethyl methacrylate. Basically, all test materials were polymerized in accordance with the manufacturer's instructions. As no guidelines were indicated on the powder to liquid ratio for Duralay and it should be more accurate when measured by weight rather than volume, the powder to liquid ratio was maintained to 2:1 by weight. In this ratio, the three resins showed similar pourable consistency after mixing for 15 seconds.

Mold Fabrication for Polymerization

A brass master mold with an inner butt-joint cavity was made. Outer dimensions of the cavity were 40.0mm(length), 25.0mm(width), and 5.0mm(depth) as illustrated in Fig. 1a. Two side troughs (left and right side to the cavity) were designed to install a strain gauge and a thermocouple within the cavity as shown in Fig. 1a. Two additional troughs (upper and lower side to the cavity) were also prepared to provide an escape way for excess resin material. All axial surfaces of a cavity had a 10-degree taper to ensure easy removal of the specimen after completing polymerization.

A polyvinyl siloxane(Exaflex, GC Inc., Japan) impression of the brass master mold was taken to du-

Table Ⅰ. Types and manufacturers of three autopolymerizing acrylic resins evaluated

Resin	Composition	Manufacturer
Duralay	Poly(methyl methacrylate)	Reliance Dental Mfg.Co.,Worth, Illinois, U.S.A.
Snap	Vinyl ethyl methacrylate	Parkell, Farmingdale, New York, U.S.A.
Vertex	Poly(methyl methacrylate)	Dentimax, Zeist Holland

plicate stone replicas of the brass master mold. After the impression material set, the mold replicas were fabricated by repeated pouring of type Ⅲ dental stone. Additionally, lids with the same external dimension as the mold replica were also fabricated (Fig. 1b). All resin-contacting surfaces of both mold replicas and lids were as highly polished as possible using up to 1000-grit sandpaper so that possible mechanical interlocking with uncured resin material would be minimized. After final flushing with copious amounts of distilled water, mold replicas and lids were stored in room temperature environment (22±2℃).

Computerized Data Acquisition System for Strain and Temperature Measurement

A block diagram and actual strain and temperature measurement system were depicted in Fig. 2 and Fig. 3, respectively. In this system, strain and temperature changes were simultaneously measured and automatically recorded. A strain gauge (AE-11-S50N-120-EC, CAS Inc., Korea) and a thermocouple inside the mold replica were connected to the signal conditioning amplifier (DA1600 Dynamic Strain Amplifier, CAS Inc., Korea). Then, the analog signals from the amplifier were collected and transformed into the digital signals by an analog-digital converting equipment (AT-MIO-16E-1, National Instrument Inc. Austin, Texas, U.S.A.), which was installed in a personal computer. Finally, digital data recordings were executed by pre-programmed software (LabView version 5.1, National Instrument Inc, Austin, Texas, U.S.A.). Captured data were stored in the personal computer, which could be analyzed statistically.

Strain and Temperature Measuring Procedures

Before mixing pre-measured monomer and polymer, every exposed surface of mold replica was thoroughly coated with white petroleum jelly as a separating medium to ensure as unhindered shrinkage of resin as possible. A strain gauge and a ther-

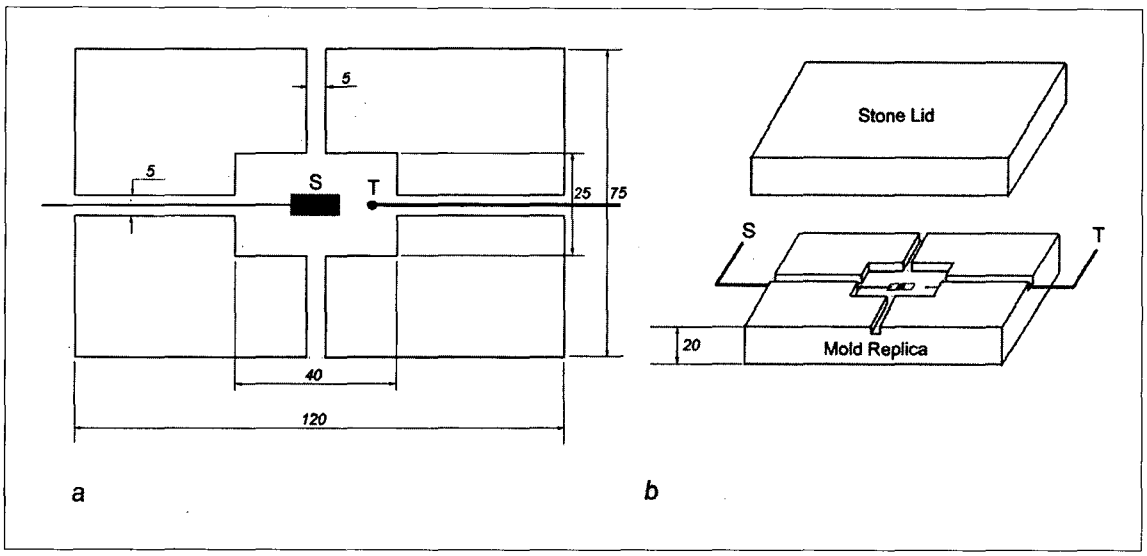

Fig. 1. Schematic illustrations of the prepared cavity in the brass master mold with the locations of sensors within the cavity (a) and the mold replica with its lid (b)
S : Strain gauge T : Thermocouple

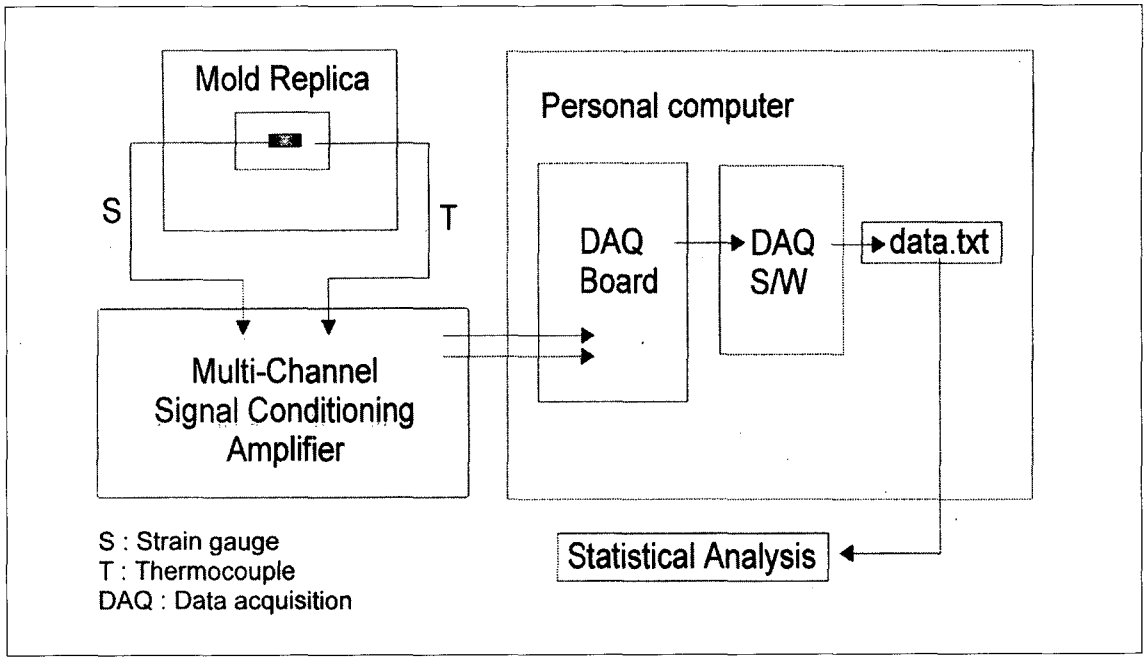

Fig. 2. Block diagram for computerized strain and temperature measurement system.

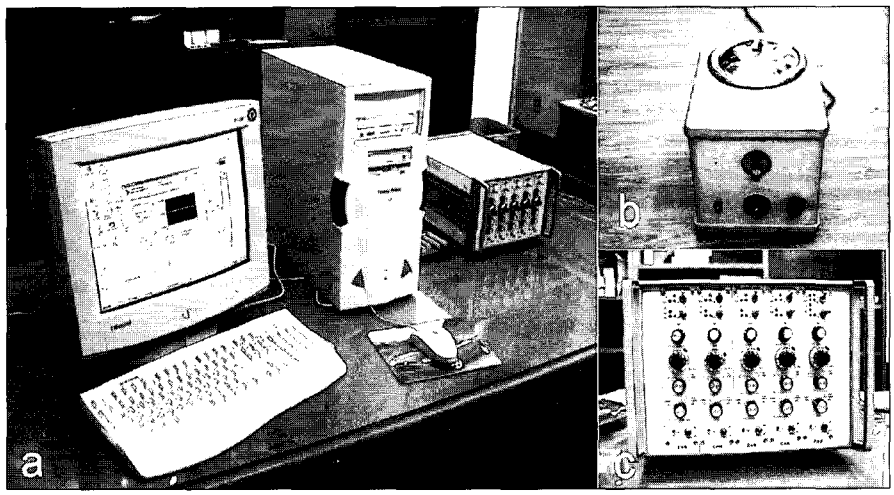

Fig. 3. Photographs of computerized data acquisition system for strain and temperature measurement.
(a) The entire computerized data acquisition system
(b) Controllable waterbath used in the third experiment (Hanau Junior Curing Unit, Model No.76-0, Teledyne Hanau, New York, U.S.A.)
(c) Multi-channel signal conditioning amplifier

mocouple were precisely positioned on the bottom surface of the cavity within the mold replica as depicted diagrammatically in Fig. 1a. Bond surface of stain gauge was in an upward direction.

Actual data recording began at the moment when the mixing procedure started. After completing a 15-

second mixing of pre-measured monomer and polymer, the fresh resin mixture was poured immediately into the mold replica that had previously accommodated a strain gauge and a thermocouple respectively, in which the polymerization process began. The output of the strain gauge and the thermocouple was connected to the signal conditioning amplifier, which had been balanced to zero. Immediately after resin pouring, the slightly overfilled mold replica was closed with a lid without additional seating force. The lid had been also coated with white petrolleum jelly before closing. The purpose of lid was to flatten the surface of resin during the polymerization reaction so that it should minimize possible vertical deformation of the resin specimen during the polymerization. In this way, strain and temperature changes were recorded at the same time during the entire polymerization up to 180 minutes. The time interval between each data recording was three seconds. Multiple runs of each material (n=10, total 30 specimens) were performed to enable statistical analysis.

The second experiment was done to evaluate the effect of removal of the resin specimen from the mold replica at the pre-determined time (15, 30 and 60 minutes from the start of mixing) during the polymerization. Initially, the lid was carefully separated from the mold replica with a light lifting force, then the resin specimen was also removed, and two sharp metallic instruments inserted into upper and lower troughs of mold replica. Once removed from the mold replica, the resin specimen continued to bench-cure in the ambient condition up to 180 minutes. Data were recorded every three second, throughout the entire 180 minutes reaction time without any interruption. Measurements were repeated 6 times for each combination of three resin materials and three removal times. Total number of specimens was 54.

In the third experiment, each specimen began its polymerization as described in the first experiment. However, at 5 minutes from the start of mixing, the entire mold assembly including its lid was put into a waterbath, that had been previously adjusted to maintain 50°C water temperature. After completing heat-soaking procedure for either 15 or 45 minutes, the mold assembly returned to the room temperature, there it continued to polymerize for up to 60 minutes from the start of the mixing. At that moment, the specimen was removed from the mold replica using the procedure described in the previous experiment. It then continued to bench-cure in the ambient condition up to 180 minutes. Measurements were repeated 5 times for each combination of three resin materials and two different heat-soaking durations. Total number of specimens in the third experiment was 30.

Strain gauge Calibration

The signal conditioning amplifier (Fig. 3) used in this study has an internal shunt calibration circuit. Therefore, additional procedures for strain gauge calibration were not necessary. Although the strain gauges used in this study had no absolute temperature compensating capability, the gauge responses were anticipated to be relatively flat, regardless of temperature changes during the exothermic reactions within the range observed in this study. For the temperature range between -12°C and 95°C, the gauge factor changes less than ± 1.0% as noted in its technical data sheet offered by the manufacturer.

Thermocouple Calibration

For converting the recorded voltage values from thermocouple to actual temperature value, the thermocouples were calibrated in the 20°C to 100°C range by repeated submersion in distilled water with a well-controlled temperature.

Data Manipulation & Statistical Analysis

The original set of recorded data for a 180-minute polymerization was voltage data. Corrected strain and temperature values were obtained on the basis of the strain gauge and thermocouple calibration.

For each experiment, important temperature and strain parameters were chosen. Then, these parameter-related data were extracted from each set of data using a spreadsheet program. Next, mean values of data were obtained for each parameter, from which time-dependent strain and temperature profiles for each experiment were constructed.

Maximum shrinkage rates were calculated for the first and third experiment from every 3-second interval strain data for each polymerization, which translates to the highest shrinkage strain change per second during 180-minute polymerization. Strain changes after removal were calculated in the second experiment, which means the differences of measured shrinkage strains between the time immediately before the removal and one minute after it. Linear thermal expansion coefficients were calculated in the third experiment using strain and temperature data from the end of heat soaking for each duration.

For several important parameters, the significant differences were examined by one-way analysis of variance (ANOVA) and the exact source of the differences was identified by the Duncan' s multiple range tests.

RESULTS

A typical time-dependent strain and temperature profile during the 180-minute polymerization observed in the first experiment is shown in Fig. 4. This graphical representation is constructed from the mean values of several critical parameters shown in Table Ⅱ and Table Ⅲ.

Strain and temperature profiles obtained from ten specimens were quite similar for each material. The origin of the horizontal axis corresponds to the moment at which mixing started. Mean measurements of several critical parameters for each material are shown in Table Ⅱ and Table Ⅲ, respectively. The parameter S_t means a measured strain for a given time t. The parameter ES means an expansion strain for a given time and ES_{max} indicates the maximum expansion strain measured. The unit

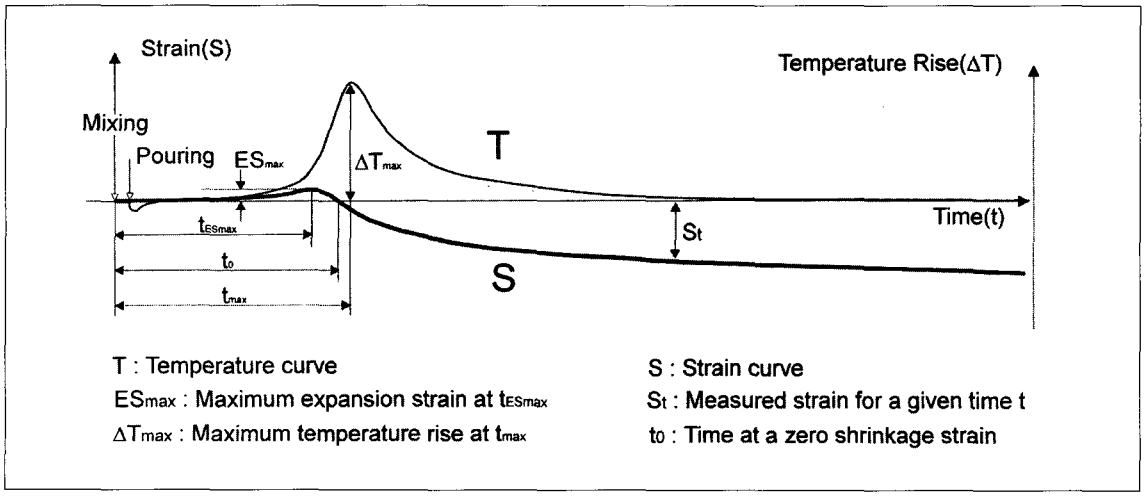

Fig. 4. Typical time-dependent profile of strain and temperature changes with characteristic parameters being displayed in the first experiment.

for strain value is microstrain ($\mu\varepsilon$).

All the data for ΔT_{max}, S_{180}(Strain at 180 minutes), and MSR shown in Table Ⅱ and Table Ⅲ were compared statistically with an one-way analysis of variance (ANOVA). Exact source of the differences were also identified by the Duncan's multiple range test.

Measured ΔT_{max} for each material at the time tmax are depicted in Fig. 5. The mean values of ΔT_{max} reached 56.7℃, 41.3℃ and 56.1℃ for Duralay, Snap, and Vertex, respectively. Snap material showed significantly lower temperature rise at its exothermal peak ($p<0.01$) (Table 1, 2).

Shrinkage strains at 180 minutes for each material are compared in Fig. 6. The mean shrinkage strain reached -3095$\mu\varepsilon$, -1796$\mu\varepsilon$ and -2959$\mu\varepsilon$ for Duralay, Snap, and Vertex, respectively as shown in Table Ⅲ. Snap produced significantly less shrinkage strains at the end of 180-minute polymerization ($p<0.01$) (Table 3, 4).

As shown in Table Ⅲ, mean MSR for each resin was calculated to -31.8$\mu\varepsilon$/sec, -15.9$\mu\varepsilon$/sec and -

Table Ⅱ. Mean measurements of time and temperature parameters in the first experiment

Resin	n	t_{ESmax}(sec)	t_0(sec)	t_{max}(sec)	ΔT_{max}(℃)
Duralay	10	461	525	520	56.7
Snap	10	448	508	502	41.3
Vertex	10	459	510	512	56.1

Table Ⅲ. Mean measurements of strain parameters in the first experiment ($\mu\varepsilon$)

Resin	n	ES_{max}	MSR* ($\mu\varepsilon$/sec)	S_{15}	S_{30}	S_{60}	S_{120}	S_{180}
Duralay	10	547	-31.8	-2384	-2600	-2845	-2978	-3095
Snap	10	423	-15.9	-1373	-1605	-1684	-1746	-1796
Vertex	10	593	-31.8	-2298	-2536	-2718	-2809	-2959

* MSR : Maximum shrinkage rate

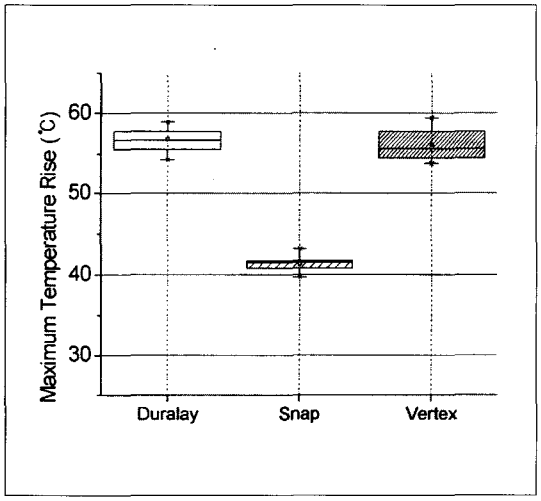

Fig. 5. Comparison of Maximum Temperature Rise (ΔT_{max}) among three resin materials in the first experiment.

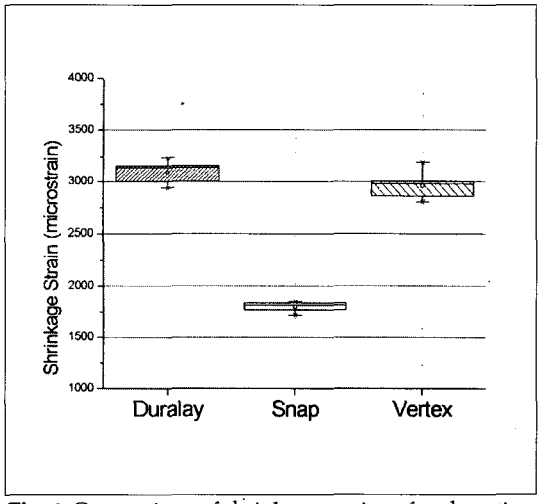

Fig. 6. Comparison of shrinkage strains of each testing material at 180 minutes (S_{180}) in the first experiment.

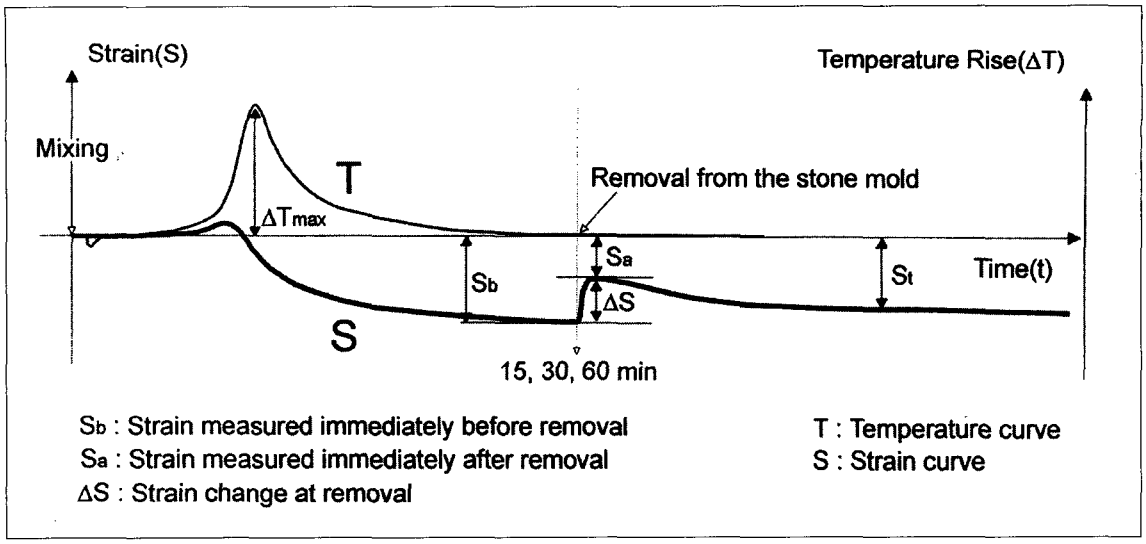

Fig. 7. Typical time-dependent profile of strain and temperature changes with characteristic parameters being displayed in the second experiment.

Table Ⅳ. Mean measurements of strain parameters in the second experiment ($\mu\varepsilon$)

Resin	R time*	n	ΔS	S_b	S_a	S_{60}	S_{120}	S_{180}
Duralay	15	6	823	-2453	-1628	-2459	-2615	-2707
	30	6	1016	-2585	-1569	-2069	-2291	-2434
	60	6	1174	-2876	-1701	-2876	-2264	-2454
Snap	15	6	599	-1370	-764	-916	-981	-1071
	30	6	782	-1611	-829	-1065	-1099	-1153
	60	6	822	-1678	-868	-1678	-1274	-1357
Vertex	15	6	669	-2369	-1700	-2640	-2861	-2995
	30	6	865	-2523	-1658	-2190	-2556	-2650
	60	6	960	-2746	-1786	-2746	-2659	-2857

* Removal time (min)

31.8$\mu\varepsilon$/sec for Duralay, Snap and Vertex, respectively. Snap showed significantly lower maximum shrinkage rates than the other two materials ($p<0.01$) (Table 5, 6).

A typical time-dependent strain and temperature profile during the 180-minute polymerization observed in the second experiment is shown in Fig. 7. This graphical representation is constructed from the mean values of several critical parameters shown in Table Ⅳ.

ΔS values were calculated from measured S_b and S_a data. Positive strain changes were always found after the removal procedure regardless of the removal time. All the data for ΔS in Table Ⅳ were compared statistically as an ANOVA and the exact source of the differences were identified by the Duncan' s multiple range test.

For each resin material, except Snap, ΔS increased with increasing removal time as depicted in Fig. 8 ($p<0.05$) (Table 7-10). For Snap, no statistical difference was found between 30 minutes and 60 minutes removal time ($p>0.05$) (Table 11,12).

For the same removal time, ΔS increased in the following order: Snap, Vertex, Duralay as shown in Fig.

8 ($p<0.05$) (Table 13-18).

As shown in Table Ⅳ, shrinkage strains at 180 minutes(S_{180}) for each material were generally lower than those observed in the first experiment. Snap showed significantly less shrinkage strains regardless of the removal time ($p<0.05$) (Table 19-24).

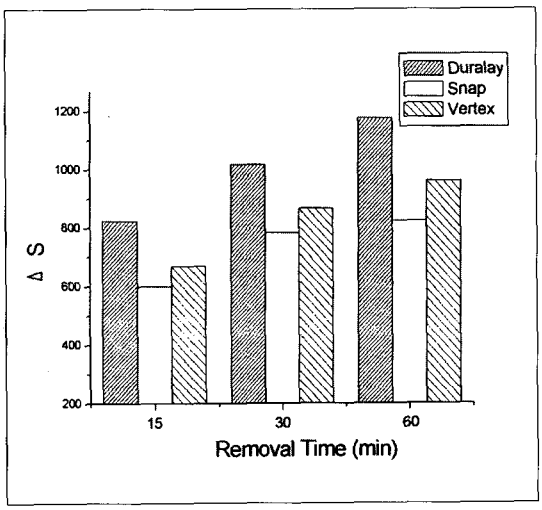

Fig. 8. Comparison of ΔS values of each resin material for three removal times in the second experiment.

A typical time-dependent strain and temperature profile during the 180-minute polymerization observed in the third experiment is shown in Fig. 9. This graphical representation is constructed from the mean values of several critical parameters shown in Table Ⅴ and Table Ⅵ.

As shown in Table Ⅴ, more elevated ΔT_{max} and additional thermal peak designated to ΔT_{max2} were uniformly observed. Unlike the values of ΔT_{max}, little differences in ΔT_{max2} were found among the resin materials within the same heat-soaking regime. It was shown that abrupt shrinkage strain after the time tESmax turned its direction into the expansion at the time t_{Sh1} as depicted in Fig. 9. These decreases in shrinkage strain continued gradually as the internal temperature of the resin reached ΔT_{max2}. At this moment, minimum shrinkage strains(for Duralay and Vertex) or even large amounts of expansion (positive) strains(for Snap) were found (Table Ⅵ). For 45-minute heat-soaking duration, higher ΔT_{max2} and more profound decreases in shrinkage strain were observed than those for 15-minute duration.

As shown in Table Ⅲ and Table Ⅵ, MSR's for

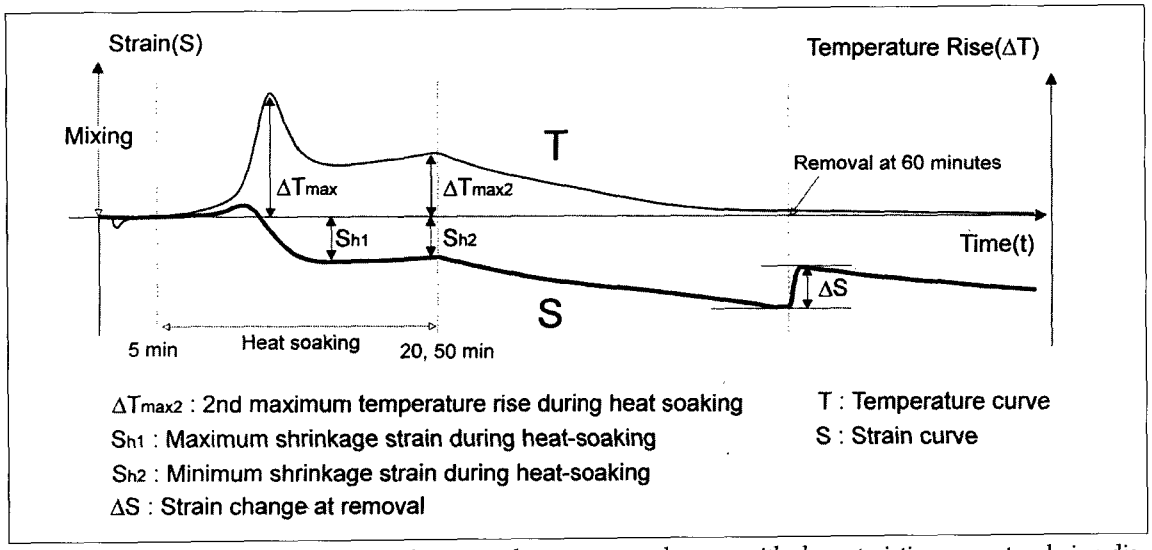

Fig. 9. Typical time-dependent profile of strain and temperature changes with characteristic parameters being displayed in the third experiment.

Table Ⅴ. Mean measurements of time and temperature parameters in the third experiment (sec)

Resin	Heating Time (min)	n	t_{ESmax}	t_0	t_{max}	ΔT_{max}(℃)	t_{max2}	ΔT_{max2}(℃)	t_{sh1}
Duralay	15[a]	5	562	625	623	66.0	1200	43.1	727
	45[b]	5	567	633	623	66.2	2605	49.9	706
Snap	15	5	561	2200	616	56.1	1200	44.8	692
	45	5	558	4378	614	55.9	1822	51.2	689
Vertex	15	5	571	614	579	72.4	1200	44.9	871
	45	5	574	617	580	73.1	2515	53.1	883

[a]*from 5 to 20 minutes from the start of the mixing*
[b]*from 5 to 50 minutes from the start of the mixing*

Table Ⅵ. Mean measurements of strain parameters in the third experiment ($\mu\varepsilon$)

Resin	Heat-soaking Time(min)	n	ES_{max}	MSR*($\mu\varepsilon$/sec)	S_{h1}	S_{h2}	LTEC**	S_{180}
Duralay	15	5	777	-31.8	-1205	-1005	81.26	-2045
	45	5	767	-31.8	-1155	-406	84.92	-2278
Snap	15	5	636	-15.9	258	616	49.56	-1003
	45	5	658	-15.9	229	1125	48.67	-525
Vertex	15	5	777	-31.8	-1136	-1112	70.96	-2417
	45	5	776	-31.8	-1071	-862	69.63	-2694

**Maximum shrinkage rate($\mu\varepsilon$/sec)*
***Linear thermal expansion coefficient(unit : 10^{-6}/℃)*

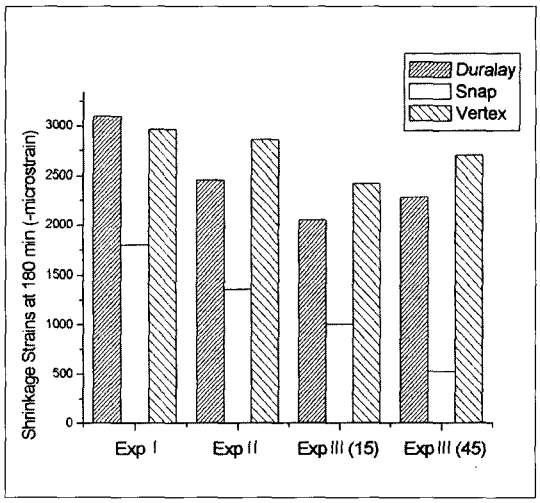

Exp Ⅰ : Experiment Ⅰ
Exp Ⅱ : Experiment Ⅱ (removal at 60 minutes)
Exp Ⅲ(15) : Experiment Ⅲ(15 minutes heat-soaking)
Exp Ⅲ(45) : Experiment Ⅲ(45 minutes heat-soaking)

Fig. 10. Comparison of shrinkage strains at 180 minutes (S_{180}) among the experiments.

each resin in the third experiment were not changed from those for the first experiment in spite of elevated ΔT_{max}.

Just after the completion of heat soaking, both internal temperature and strain were found to have gradually decreased in a linear manner as shown in the straight portion of the strain and temperature profiles in Fig. 9. Mean LTEC (linear thermal expansion coefficients) for each resin, which were calculated from the end of heat-soaking for additional 5 minutes, are shown in Table Ⅵ. Snap showed significantly lower mean LTEC than those of the other two materials for both heat-soaking regimes ($p<0.01$) (Table 25-28). Meanwhile, no significant differences were found between the mean LTEC' s from two different heat-soaking regimes by paired t-test ($p>0.05$).

In Fig. 10, for Duralay and Vertex, S_{180} in the third experiment were slightly lower than those of the first and the second experiment for both heat-soaking regimes. Snap showed significantly low-

er S_{180} values for both heat-soaking regimes ($p<0.01$) (Table 29-32).

DISCUSSION

In this study, the strain and temperature change resulting from polymerization reaction within the autopolymerizing resins were examined by the strain gauge method. Strain gauge method can be classified as one of the linear measurement methods for polymerization shrinkage determination.[8] All linear measurement methods use various electronic sensors to record time-dependent changes of polymerization shrinkage. Shrinkage determinations where the sensors require activation by way of force can only monitor the "post-gel" part of the curing contraction, when the material shows sufficient elastic modulus and is strong enough to exert forces that can activate them. Therefore, for different types of sensors, the characteristics of a sensor device determine the actual transformation of contraction into force. The less displacement needed for producing forces, the more realistic the readings.[12] Considering relatively low initial viscosity of freshly mixed autopolymerizing acrylic resins used, it is apparent that the strain data obtained in this study do not include pre-gel curing contraction of each resin.

Mostly, related articles that adopted a linear measurement method dealt with various composite resins including chemically activated materials in some occasions. Composite materials are more advantageous in experimental setup, because they already have relatively good initial viscosity owing to the presence of filler particles. For the same reason, shaping and fitting of the material into the mold can also be easier than autopolymerizing acrylic resins, which have practically fluid characteristics during the initial polymerization. Davidson et al.[16] used a tensilometer to investigate the development of the composite-dentin bond strength in relation to the polymerization shrinkage stress in linear model. They studied a chemically activated as well as a light-activated microfilled composite. Davidson et al.[12] measured with a tensilometer the hardening stresses in wall-to-wall bonded composites and related them to calculated values obtained from freely shrinking materials. Feilzer et al.[17] studied the setting stress in composite resins as a function of restoration shape with tensilometer-type displacement transducer. De Gee et al.[18] introduced the linometer device, which was originated by Feilzer et al.[19] to measure linear polymerization shrinkage of both unfilled resins and composites. Fano et al.[20] recently used a He-Ne scanning laser beam to measure the linear shrinkage of light-cured composites. Alster et al.[21] used a tensilometer for measuring the curing stress as a function of composites layer thickness. Watts et al.[22] used 'bonded disk' measurement device to measure shrinkage strain of composite materials from initial irradiation. It was concluded that the bonded disk shrinkage-strain measurement technique is suitable for the elucidation of such rapid kinetic and temperature-dependent events during the photo-polymerization setting process.

Contrary to these linear shrinkage determination methods, volumetric curing contraction determination can be described as basically "free" shrinkage measurements, which can offer the total (pre- and post-gel) curing contraction. Mercury-filled dilatometry was a typical method that could be classified into this category and has been used widely in many articles.[23-28] Water-filled dilatometry[15,29-33] was developed and subsequently used to remove the disadvantage of using toxic mercury. Cook et al.[34] described a gas pycnometer, which was a non-contact method and was appropriate for shrinkage measurements where only the total amount of shrinkage was required. This method was also regarded to be particularly useful for the measurement of shrinkage of light-activated materials which are sensitive to water absorption.

Strain gauge method has been widely used in recent dental literature. Stafford et al.[35] investigated the strain levels obtained on poly(methyl methacry-

late) dentures to calculate the magnitude and direction of the principal strain in the denture bases during biting and swallowing. The majority of studies were focused on the composite materials. Donly et al.[36] attached precision strain gauge to the buccal surface of the tooth to evaluate cuspal strain changes under the influences of various polymerization schemes for posterior composite resin. Sakaguchi et al.[9] monitored the polymerization contraction of composite restoratives to verify the accuracy and efficacy of the strain gauge methodology. It was concluded that the strain gauge method appeared to be well suited for real-time measurement of the curing process and provided a means for studying the kinetics of polymerization. Sakaguchi et al.[10] introduced more advanced experimental setup for the strain gauge method. By using a surrounding acrylic ring and two strain gauges, the calculation of contraction stress was possible by measuring contraction strain of the ring in real-time. Versluis et al.[11] determined the thermal expansion coefficient for seven commonly used restorative resin composites by measuring the instantaneous strain along with temperature change. Meredith et al.[37] measured changes in cuspal strain and displacement occurring during placement and polymerization of bonded composite restorations in extracted human teeth in vitro. Recently, Komiyama et al.[14] investigated residual stress relaxation in heat-activated acrylic denture base resin fabricated by the polymer-monomer mixture method. Thermocouples and strain gauges were embedded in resin for measuring temperature and strain from the dough-stage of resin packing. To clarify the stress relaxation in the mold replica, specimens were removed from the mold by deflasking. Kawara et al.[13] reported qualitatively on polymerization and thermal shrinkage factors in heat-activated acrylic denture base resins. The results revealed that the shrinkage of heat-activated acrylic denture base resin was mainly thermal shrinkage, and demonstrated the advantage of the low-temperature method in reducing thermal shrinkage.

After the initial contact between a fresh resin mixture and sensors, both temperature and strain gradually increased with positive values up to the value of ES_{max} for the time t_{ESmax}, indicating temperature rise and expansion strain as shown in Fig. 4. These expansion strains were uniformly measured. Strain gauges are symmetrical in that they can record expansion as accurately as shrinkage, and generally the performance characteristics of the gauges apply equally well to both positive and negative linear change. The three resin materials in this study showed almost identical patterns of expansion strains before the maximum temperature rise (ΔT_{max}) occurred. These observations also bear a close resemblance to the results previously reported on light-activated composite resin materials9 and heat-activated denture base materials.[13,14] Substantially, expansion strains found in this period are considered the net results of interactions between the shrinkage strains generated from the polymerization and the expansion strains generated from thermal expansion of the specimen.

When the reaction time reached t_{max}, the temperature rises showed maximum values as shown in Table Ⅱ. Snap is shown to produce significantly lower temperature rise than the other two materials (Fig. 5). It is postulated that the different chemistry(vinyl ethyl methacrylate) of Snap is the major cause of the difference. The difference of reaction exotherm between poly(methyl methacrylate) and other chemical compounds has been reported.[38-40] In those studies, poly(methyl methacrylate)' s temperature rises were significantly higher than those of the other materials including vinyl ethyl methacrylate. Generally, the chemical composition of acrylic resin affects the temperature rise at the time of polymerization.[40] For Duralay and Vertex, which are based on the same chemistry, the heat generation during the polymerization of a commensurate amount of material may be assumed to be approximately equal, since the same quantity of monomer undergoes polymerization.

During the polymerization reaction, bond dissociation energy is released from the polymer,[41] which causes the comparable temperature elevation. Many investigators have published the influence of heat on the dental pulp. A classical report by Pohto et al.[42] showed the following effects of temporary heating or cooling of a tooth on the pulp vessel system from the temperature of 37℃:31℃, decrease of blood flow rate;42℃, increase of blood flow rate;42 ℃ to 44℃, permeability increase with edema;44℃ to 46℃, tendency for erythrocyte aggregation;46 ℃ to 60℃, stasis and thrombosis. In experiments with monkeys, it was demonstrated that irreversible injury occurs with temperature elevations exceeding 5.5℃.[43] An early study on dogs showed that pulp recovery with reparative dentin formation occurred after the intrapulpal temperature rose more than 25 ℃.[44] Grajower et al.[45] measured the temperature rise in the pulp chamber of incisors during the curing of temporary crowns on tooth preparations. It was reported that heat dissipation due to blood circulation in the pulp is probably not effective during the curing of temporary crowns on incisors. Moulding et al.[46] compared the heat transferred to the pulp by different types of resin, quantities, and matrices commonly used in fabricating direct extracoronal provisional restorations. It was shown that Duralay induced the greatest temperature increase. Snap also showed less temperature increase than Duralay, similar to the results of the present study. Driscoll et al.[38] evaluated the heat-producing capabilities of poly(methyl methacrylate), vinyl ethyl methacrylate, visible-light activated resin, and bis-acrylic composite resin. Poly(methyl methacrylate)' s temperature increases were significantly higher than those of the other three materials. Chirtoc et al.[47] investigated four groups of autopolymerizing acrylic resins used for various purposes in current dental practice by monitoring their temperature changes during the polymerization process. It was noted that products with lower temperature production would solidify first. Vallittu[40] determined peak temperatures of some prosthetic acrylic resins at the time of polymerization using a thermocouple. It was shown acrylic resins for temporary restorations had lower peak temperatures than those for other purposes. However, despite the lower peak temperature, the temperature of resins for temporary restoration can be as high as 82℃ during polymerization. In the present study, the mean maximum temperature rise for Vertex was about 56℃ in the first experiment. Considering the room temperature(22±2℃), this result closely resembles that of Vallittu. Castelnuovo et al.[48] also demonstrated that the amount of heat generated during resin polymerization and transmitted to the pulpal chamber could be damaging to pulpal tissues including odontoblast. Though some authors including Baldissara et al.[49] maintained the opposite point of view on this subject, it is still general agreement that effective cooling procedure should be prepared when using autopolymerizing acrylic resins intraorally. In this study, Snap showed significantly lower maximum temperature rise than Duralay and Vertex. Even the lowest temperature rises for Snap, however, are still beyond the known temperature tolerance level of oral mucosa and pulp tissue. Tooth insulation with a sort of coating or employing the indirect method has been recommended for intraoral manipulation of autopolymerizing acrylic resins.[50]

In Fig. 6, at 180 minutes from the start of mixing, the shrinkage strain of Snap was significantly less than that of both Duralay and Vertex in the first experiment. To evaluate this result, it must be considered that the elastic modulus of polyvinyl acrylic is known to be about two-thirds that of poly(methyl methacrylate).[51] A material with lower elastic modulus has the general tendency to show less deformation or strain at the same stress level. Therefore, it can be assumed that internal stresses during the polymerization caused less overall shrinkage strain in Snap than the two other materials. The second point of view concerns the thermal expansion property of resin material. Lower thermal coefficient of ex-

pansion of polyvinyl acrylic material[51] could possibly be the second contributing factor explaining the lower shrinkage strain of Snap. No statistical difference was found in the shrinkage strain at 180 minutes between two poly(methyl methacrylate) products.

It has been reported that polymerization shrinkage occurred mainly during the first 3hours(approximately 0.4% linear) by the combined method using a dilatometer and a linear inductive transducer.[15] With the same study, 80% of all the polymerization shrinkage occurred before 17 minutes for Duralay and Palavit G resins, and 95%, before 3 hours for Duralay and 2 hours for Palavit G resins. In this study, it was also found that the ratio of S_{15} to S_{180} can be calculated to 77.02%, 76.44%, and 77.66% for Duralay, Snap, and Vertex respectively on the basis of the values in Table Ⅲ. This means that about 80% of polymerization shrinkage occurs before 15 minutes polymerization as compared with that of 180 minutes.

In the second experiment, positive strain change was uniformly found in each resin specimen regardless of the removal time. The first consideration about the strain changes found after the removal procedure in the second experiment concerns the specimen geometry in which the mold that confined the resin allowed it to contract freely without any chemical or mechanical bond between the mold and resin specimen cured. Davidson et al.[8] assumed that in a situation where a curing material is bonded on all sides to rigid structures, bulk contraction is impossible and all shrinkage must be compensated for by some kind of volume generation. In that situation, a shrinkage strain on the material itself is minimal. It was also noted that the volume generation could come mainly from dislodgement of the bond, increase in porosity or internal loss of coherence. In this particular case, all shrinkage must be regarded as a possible contribution to stress. Feilzer et al.[17] defined the configuration factor as the ratio of the bonded to the unbonded surfaces of the restoration. They were able to demonstrate experimentally that there is a relationship between configuration and stress development. Taking into account this consideration, the resin specimen under autopolymerization in this experiment had no bond on every surfaces to the inner mold space and then bulk contraction could be maximized.[52] Majority of thermal and polymerization contraction stresses can be transformed into the shrinkage strains in this type of unbonded specimen geometry, except for those which have non-horizontal direction, owing to the presence of confinement provided by the mold space and the lid that covers the entire upper surface of a mold replica.

The second consideration to explain the true nature of ΔS values (Fig. 7) observed is the location and direction where the strain gauge is installed within the mold cavity in this study. As illustrated in Fig. 1b, the strain gauge was fixed on the bottom surface of the 5.0mm-depth mold cavity. Generally, the measuring surface of a strain gauge should always face toward the target material tested. In this study, it was necessary that the strain gauge should be installed with its the measuring surface toward the resin cured. Accurate measurements are not guaranteed if the opposite surface of the strain gauge is toward the resin, because the backing surface of the strain gauge does not have the necessary surface roughness to ensure enough mechanical bond between the target material and the strain gauge. Therefore, considering this unavoidable limitation of the gauge attachment, it can be postulated that positive ΔS values should accompany some lengthening of the bottom surface of the resin specimen.

The third consideration when analyzing the strain changes found in the second experiment is related to the stress generated during the polymerization. When acknowledging the presence of the inhibition created by the spatial confinement of the mold replica, it can be postulated that non-horizontal curing stresses can be inhibited, so that it cannot be transformed into measurable strains until the resin specimen is completely removed from the mold

that has confined it. During the actual removal procedure done in the second experiment, it was also found that initial removal of the lid produced little change in strain value but complete removal from the mold induced most of the strain changes. With the considerations of the specimen geometry and the gauge direction, ΔS values observed in the second experiment can be related to the possible bending deformation of the specimen, caused by non-horizontal curing stresses that were not transformed into the measurable strains owing to the confinement created by the mold assembly.

As summarized in Table Ⅳ, it was also found that strains measured after one minute from the removal procedure (S_a) had quite similar for each resin material, regardless of the removal time. For longer duration of curing time before the removal procedure, S_b values increased correspondingly as observed in the first experiment. But, if the specimen was removed from the mold assembly, more decrease of shrinkage strain from S_b occurred in the specimen that has been cured for longer duration. Consequently, as the removal time increased, greater ΔS value was produced for each resin material as shown in Fig. 8.

The mean shrinkage strains at 180 minutes (S_{180}) of each material in the second experiment were generally lower than those of the first experiment as compared in Table Ⅲ and Table Ⅳ. Snap showed significantly less shrinkage strains for all three removal times. In addition to S_{180} values, the calculated differences between the values of S_a and S_{180} were far less than those of Duralay and Vertex. This means that after the removal procedure, Snap material developed the smallest additional shrinkage strains. This finding corresponds to the result of the first experiment (Fig. 12).

Being different from the previous two experiments, the second thermal peak(ΔT_{max2}) was found during the third experiment. This additional temperature rise was definitely produced by the heat supplied by the waterbath. The experimental design adapted in this experiment can effectively minimize well-known expansion effect of water submersion of a resin material.[53] White petrolleum jelly that had been previously coated on the entire contact surface of the mold assembly served to minimize the possible invasion of water in the specimen during the heat-soaking period.

For both heat-soaking durations, the first thermal peaks showed higher temperature rises than those from the previous two experiments. The second thermal peaks were recorded at almost the same temperature levels for each heat-soaking duration, regardless of resin materials. Higher ΔT_{max2} were always recorded in 45-minute heating group than those in 15-minute heating group (Table Ⅴ). Under the influence of this external heat supply, all of the values for parameter ES_{max}, t_{ESmax}, t_{max} were increased.

The most pronounced findings during the heat-soaking procedure were dramatically diminished early shrinkage strains after the maximum temperature rises. Decrease of shrinkage strain was uniformly found at the time t_{sh1}, instead of abrupt and continuous production of shrinkage strains as observed during the first and second experiments. Those gradual expansion strains were recorded from S_{h1} to S_{h2} with straight portions as shown in Fig. 9. Snap even showed absolute positive strains, which means that for the entire heat-soaking period, no negative strains indicating shrinkage were found for Snap, regardless of heat-soaking duration.

Although three resin materials have showed similar ΔT_{max2} at the end of heat-soaking procedure, final shrinkage strains at 180 minutes for Snap were far smaller than those for Duralay and Vertex. (Table Ⅵ, Fig. 10). As shown in Table Ⅵ, the maximum shrinkage rates for each material were not changed in the third experiment as compared to the data found in the first experiment. This means that additional heat supply did not alter the speed of shrinkage at the moment of the highest temperature rise. This also shows that the major factor governing polymerization reaction in that early period of

the reaction is polymerization contraction which came mostly from actual polymerization of monomer, and not the thermal contraction induced by temperature downfall from the thermal peak. In this study, the maximum shrinkage rate for Snap is about half of that for Duralay and Vertex. In the case of Snap, it can be suggested that much lower maximum shrinkage rate played an important role in producing lower polymerization shrinkage after 180 minutes.

The second consideration for lower shrinkage strain of Snap concerns the much lower thermal expansion coefficient of Snap obtained after the heat-soaking period. Materials with lower thermal expansion coefficient have a tendency to expand or shrink less for a given temperature change than those with higher value. After completing the heat-soaking with the internal temperature of ΔT_{max2} and the strain S_{h2} accordingly, gradual decreases of both temperature and strain were found in a linear nature as shown in Fig. 9. Thermal expansion coefficient of each material can be calculated from those straight portions of the profile. In fact, the coefficients that were calculated in this period are not exact values, since complete polymerization reaction had not occurred yet at that time. Estimated coefficients here include some portion of polymerization shrinkage not finished at that time, especially for 15-minute heating group. In Table Ⅵ, it is shown that the thermal expansion coefficients of Duralay and Vertex are much greater than those of Snap. In general, thermal expansion coefficient for poly(methyl methacrylate) is known $81 \times 10^{-6}/^{\circ}C$.[6] That corresponds well to the calculated values for Duralay and Vertex (approx. $80 \times 10^{-6}/^{\circ}C$ and $70 \times 10^{-6}/^{\circ}C$, respectively) in this study. Unfortunately, no published data are currently available for vinyl ethyl methacrylate.

In Table Ⅵ, no significant differences were found between the linear thermal expansion coefficients obtained from the two heat-soaking durations. In other words, the linear thermal expansion coefficients calculated from the strain and temperature data at 20-minute progression of the polymerization were not different from those at 50-minute progression. If one considers the strain and temperature profiles found in the first experiment, it can be positively concluded that the polymerization shrinkage from actual polymerization of monomer has little influence on the overall shrinkage generated after an abrupt shrinkage near the maximum temperature rise.

As compared to the ΔS values of the second experiment with the corresponding removal time, the mean ΔS values in the third experiment can be seen to have generally decreased as shown in Table Ⅵ. It was previously suggested that the observed ΔS values could be related to the possible relaxation of non-horizontal curing stress. In the third experiment, internal temperature of resins were elevated and maintained for a relatively long period of time. It may be possible that some molecular reorientation or internal polymer chain remodelling occurred to reduce stress accumulation.

More sophisticated design of devices and methods should be developed to fully understand the entire mechanism governing polymerization shrinkage behavior of autopolymerizing acrylic resins so that the development and clinical usage of the ideal material with no shrinkage could be possible in the near future.

CONCLUSIONS

Within the limitations imposed by the selection of materials and the conditions of the study, the following conclusions may be made:

1. The mean shrinkage strains reached -3095$\mu\varepsilon$, -1796 $\mu\varepsilon$ and -2959$\mu\varepsilon$ for Duralay, Snap and Vertex, respectively. The mean maximum temperature rise reached 56.7℃, 41.3℃ and 56.1℃ for Duralay, Snap, and Vertex, respectively. A vinyl ethyl methacrylate product (Snap) showed significantly less polymerization shrinkage strain ($p<0.01$) and significantly lower maximum tem-

perature rises ($p<0.01$) than the other two poly(methyl methacrylate) products (Duralay, Vertex).

2. Mean maximum shrinkage rate for each resin was calculated to -31.8$\mu\varepsilon$/sec, -15.9$\mu\varepsilon$/sec and -31.8 $\mu\varepsilon$/sec for Duralay, Snap and Vertex, respectively. Snap showed significantly lower maximum shrinkage rate than Duralay and Vertex ($p<0.01$).
3. Positive strain changes were found after the removal of specimen from the mold, and the amount of changes increased as the removal time was delayed. For each removal time, Snap showed significantly less strain changes than the other two poly(methyl methacrylate) products ($p<0.05$).
4. During the external heat supply for the resins, higher maximum temperature rises were found. Meanwhile, the maximum shrinkage rates were not different from those of room temperature polymerizations.
5. The external heat supply for the resins during polymerization could temporarily decrease or even reverse shrinkage strains of each material. But, shrinkage re-occurred in the linear nature after completion of heat supply.
6. Linear thermal expansion coefficients obtained from the end of heat supply continuing for an additional 5 minutes, showed that Snap exhibited significantly lower values than the other two poly(methyl methacrylate) products ($p<0.01$). Moreover, little difference was found between the mean linear thermal expansion coefficients obtained from two different heating durations ($p>0.05$).

REFERENCES

1. J. Mondelli, A.C. Piccino and A. Berbert An acrylic resin pattern for a cast dowel and core. J Prosthet Dent 1971;25:413-417.
2. N. Stern A direct pattern technique for posts and cores. J Prosthet Dent 1972;28:279-283.
3. G.C. Cho and W.W. Chee Efficient soldering index materials for fixed partial dentures and implant substructures. J Prosthet Dent 1995;73:424-427.
4. J.C. Patterson A technique for accurate soldering. J Prosthet Dent 1972;28:552.
5. K.J. Anusavice: Philips' Science of Dental Materials, 10th ed. Philadelphia, WB Saunders Co, 1996, p213.
6. R.G. Craig and M.L. Ward: Restorative Dental Materials, 10th ed. St. Louis, Mosby-Year Book, Inc, 1997, p511.
7. M.P. Patel, M. Braden and K.W.M. Davy Polymerization shrinkage of methacrylate esters. Biomaterials, 1978;8:53-56.
8. C.L. Davidson and A.J. Feilzer Review. Polymerization shrinkage and polymerization shrinkage stress in polymer-based restoratives. J Dent 1997;25:435-440.
9. R.L. Sakaguchi, C.T. Sasik, M.A. Bunczak and W.H. Douglas Strain gauge method for measuring polymerization contraction of composite restoratives. J Dent 1991;19:312-316.
10. R.L. Sakaguchi, M.C.R.B. Peters, S.R. Nelson,W.H. Douglas and H.W. Poort Effects of polymerization contraction in composite restorations. J Dent 1992;20:178-182.
11. A. Versluis, W.H. Douglas, and R.L. Sakaguchi Thermal expansion coefficient of dental composites measured with strain gauges. Dent Mater 1996;12:290-294.
12. C.L. Davidson and A.J. de Gee Relaxation of polymerization contraction stresses by flow in dental composites. J Dent Res 1984;63:146-148.
13. M. Kawara, O. Komiyama, S. Kimoto, N. Kobayashi, K. Kobayashi, and K. Nemoto Distortion behavior of heat-activated acrylic denture-base resin in conventional and long, low-temperature processing methods. J Dent Res 1998;77:1446-1453.
14. O. Komiyama, and M. Kawara Stress relaxation of heat-activated acrylic denture base resin in the mold after processing. J Prosthet Dent 1998;79:175-181.
15. P. Mojon, J.P. Oberholzer, J.M. Meyer, U.C. Belser Polymerization shrinkage of index and pattern acrylic resins. J Prosthet Dent 1990;64:684-688.
16. C.L. Davidson, A.J. de Gee and A.J. Feilzer The Competition between the composite-dentin bond strength and the polymerization contraction stress. J Dent Res 1984;63:1396-1399.
17. A.J. Feilzer, A.J. de Gee, and C.L. Davidson Setting stress in composite resin in relation to configuration of the restoration. J Dent Res 1987;66:1636-1639.
18. A.J. de Gee, A.J. Feilzer, C.L. Davidson True linear polymerization shrinkage of unfilled resins and composites determined with a linometer. Dent Mater 1993;9:11-14.
19. A.J. Feilzer, A.J. de Gee, C.L. Davidson Increased wall-to-wall curing contraction in thin bonded resin layers. J Dent Res 1989;86:48-50.
20. V. Fano, I. Ortalli, S. Pizzi and M. Bonanini Polymerization shrinkage of microfilled composites determined by laser beam scanning. Biomaterials 1997;18:467-470.
21. D. Alster, A.J. Feilzer, A.J. de Gee, C.L. Davidson

Polymerization contraction stress in thin resin composite layers as a function of layer thickness. Dent Mater 1997;13:146-150.
22. D.C. Watts and A.A. Hindi Intrinsic 'soft-start' polymerisation shrinkage-kinetics in an acrylate-based resin-composite. Dent Mater 1999;15:39-45.
23. D.L. Smith and I.C. Schoonover Direct filling resins: dimensional changes resulting from polymerization shrinkage and water sorption. J Am Dent Assoc 1953;46:540-544.
24. A.J. de Gee, C.L. Davidson and A. Smith A modified dilatometer for continuous recording of volumetric polymerization shrinkage of composite restorative materials. J Dent 1981:9;36-42.
25. J.R. Bausch, K. de Lange, C.L. Davidson, A. Peters, and A.J. de Gee Clinical significance of polymerization shrinkage of composite resins. J Prosthet Dent 1982;48:59-67.
26. R.W. Penn A recording dilatometer for measuring polymerization shrinkage. Dent Mater 1986;2:78-79.
27. A.J. Feilzer, A.J. de Gee and C.L. Davidson Curing contraction of composites and glass ionomer cements. J Prosthet Dent 1988;59:297-300.
28. M. Iga, F. Takeshige, T. Ui, M. Torii and Y. Tsuchitani The relationship between polymerization shrinkage and the inorganic filler content of light-cured composites. Dent Mater J 1991;10:38-45.
29. S. Bandyopadhyay A study of the volumetric setting shrinkage of some dental materials. J Biomed Mater Res 1982;16:135-144.
30. M. Goldman Polymerization shrinkage of resin based restorative materials. Aust Dent J 1983;28:156-161.
31. J.N. Hay and A.C. Shortall Polymerization contraction and reaction kinetics of three chemically activated restorative resins. J Dent 1988;16:172-176.
32. J.H. Lai and A.E. Johnson Measuring polymerization shrinkage of photo-activated restorative materials by a water-filled dilatometer. Dent Mater 1993;9:139-143.
33. Yong-Keun Lee, Tae-Ho Yoon, Cheol-We Kim. A study on the polymerization shrinkage and thermal expansion fo dental esthetic restorative materials. J Korean REs Soc Dent Mater 2000;27.
34. W.D. Cook, M. Forrest, A.A. Goodwin A simple method for the measurement of polymerization shrinkage in dental composites. Dent Mater 1999;15:447-449.
35. G.D. Stafford and D.W. Griffiths Investigation of the strain produced in maxillary complete dentures in function. J Oral Rehab 1979;6:241-256.
36. K.J. Donly, T.W. Wild, R.L. Bowen, and M.E. Jensen An in vitro investigation of the effects of glass inserts on the effective composite resin polymerization shrinkage. J Dent Res 1989;68:1234-1237.
37. N. Meredith and D.J. Setchell In vitro measurement of cuspal strain and displacement in composite restored teeth. J Dent 1997;25:331-7.
38. C.F. Driscoll, G. Woolsey, W.M. Ferguson Comparison of exothermic release during polymerization of four materials used to fabricate interim restorations. J Prosthet Dent 1991;65:504-506.
39. M.B. Moulding, P.E. Teplitsky Intrapulpal temperature during direct fabrication of provisional restorations. Int J Prosthodont 1990;3:299-304.
40. P.K. Vallittu Peak temperatures of some prosthetic acrylates on polymerization. J Oral Rehabil 1996;23:776-781.
41. F.W. Billmeyer Textbook of Polymer Science. John Wiley and Sons, New York 1984, p71.
42. M. Pohto, A. Scheinin Microscopic observations on living dental pulp. Acta Odontol Scand 1958;16:303-315.
43. L. Zach and C. Cohen Pulp response to externally applied heat. Oral Surg 1965;19:515.
44. V.F. Lisanti and H.A. Zander Thermal injury to normal dog teeth: In vivo measurement of pulp temperature increases and their effect on the pulp tissue. J Dent Res 1952;31:548.
45. R. Grajower, S. Shaharbani, E. Kaufman Temperature rise in pulp chamber during fabrication of temporary self-curing resin crowns. J Prosthet Dent 1979;41:535-540.
46. M.B. Moulding, R.W. Loney The effect of cooling techniques on intrapulpal temperature during direct fabrication of provisional restorations. Int J Prosthodont 1991;4:332-336.
47. M. Chirtoc, D.D. Bicanic, M.L. Hitge, W. Kalk Monitoring the polymerization process of acrylic resins. Int J Prosthodont 1995;8:259-264.
48. J. Castelnuovo, H.L. Anthony, H.L. Tjan Temperature rise in pulpal chamber during fabrication of provisional resinous crowns. J Prosthet Dent 1997;78:441-446.
49. P. Baldissara, S. Catapano and R. Scotti Clinical and histological evaluation of thermal injury thresholds in human teeth : a preliminary study. J Oral Rehab 1997;24:791-801.
50. K. Langeland and K.L. Langeland Pulp reactions to crown preparations, impression, temporary crown-fixation and permenent cementation. J Prosthet Dent 1965;15:129.
51. R.G. Craig and M.L. Ward: Restorative Dental Materials, 10th ed. St. Louis, Mosby-Year Book, Inc, 1997, p506.
52. C.L. Davidson Resisting the curing contraction with adhesive composites. J Prosthet Dent 1986;55:446-447.
53. J.B. Woelfel, G.C. Paffenbarger, W.T. Sweeney Changes in denture during storage in water and in service. J Am Dent Assoc 1961;62:643-657.

Reprint request to:
DR. HYUNG-JUN AHN
DEPT. OF PROSTHODONTICS, COLLEGE OF DENTISITY,
SEOUL NATIONAL UNIV.
28-1 YEONGUN-DONG, CHONGNO-GU, 110-749, SEOUL KOREA
Tel:+82-2-760-2661, Fax:+82-2-760-3860
E-mail: macdds@netian.com

Table 1. Oneway ANOVA for maximum temperature rise (ΔT_{max}) in the first experiment

	Sum of Squares	df	Mean Square	F	Sig.
Between Groups	1528.161	2	764.080	316.739	.000
Within Groups	65.133	27	2.412		
Total	1593.294	29			

Table 2. Duncan' s multiple range test

Duncan[a]

		Subset for alpha = .01	
resin	N	1	2
Snap	10	41.2700	
Vertex	10		56.0800
Duralay	10		56.7200
Sig.		1.000	.365

Means for groups in homogeneous subsets are displayed.

a. Uses Harmonic Mean Sample Size = 10.000.

Table 3. Oneway ANOVA for shrinkage strains at 180 minutes (S_{180}) in the first experiment

	Sum of Squares	df	Mean Square	F	Sig.
Between Groups	10182264	2	5091132.2	586.794	.000
Within Groups	234256.974	27	8676.184		
Total	10416521	29			

Table 4. Duncan' s multiple range test

Duncan[a]

		Subset for alpha = .01		
Resin	N	1	2	3
Duralay	10	-3094.77		
Vertex	10		-2958.46	
Snap	10			-1796.41
Sig.		1.000	1.000	1.000

Means for groups in homogeneous subsets are displayed.

a. Uses Harmonic Mean Sample Size = 10.000.

Table 5. Oneway ANOVA for maximum shrinkage rates in the first experiment

MSR

	Sum of Squares	df	Mean Square	F	Sig.
Between Groups	1685.400	2	842.700		
Within Groups	8.213E-29	27	3.042E-30		
Total	1685.400	29			

Table 6. Duncan's multiple range test

Duncan[a]

Resin	N	Subset for alpha = .01	
		1	2
Duralay	10	-31.800	
Vertex	10	-31.800	
Snap	10		-15.900
Sig.		1.000	1.000

Means for groups in homogeneous subsets are displayed.

a. Uses Harmonic Mean Sample Size = 10.000.

Table 7. Oneway ANOVA for ΔS values of Duralay in the second experiment

	Sum of Squares	df	Mean Square	F	Sig.
Between Groups	371847.768	2	185923.884	55.018	.000
Within Groups	50689.510	15	3379.301		
Total	422537.278	17			

Table 8. Duncan's multiple range test

Duncan[a]

resin	N	Subset for alpha = .05		
		1	2	3
15min	6	822.6333		
30min	6		1015.8833	
60min	6			1174.1167
Sig.		1.000	1.000	1.000

Means for groups in homogeneous subsets are displayed.

a. Uses Harmonic Mean Sample Size = 6.000.

Table 9. Oneway ANOVA for ΔS values of Vertex in the second experiment

	Sum of Squares	df	Mean Square	F	Sig.
Between Groups	263708.241	2	131854.121	26.889	.000
Within Groups	73554.643	15	4903.643		
Total	337262.884	17			

Table 10. Duncan's multiple range test

Duncan[a]

resin	N	Subset for alpha = .05		
		1	2	3
15min	6	669.1667		
30min	6		865.0500	
60min	6			959.8500
Sig.		1.000	1.000	1.000

Means for groups in homogeneous subsets are displayed.

a. Uses Harmonic Mean Sample Size = 6.000.

Table 11. Oneway ANOVA for ΔS values of Snap in the second experiment

	Sum of Squares	df	Mean Square	F	Sig.
Between Groups	173747.373	2	86873.687	62.758	.000
Within Groups	20763.932	15	1384.262		
Total	194511.305	17			

Table 12. Duncan's multiple range test

Duncan[a]

		Subset for alpha = .05	
resin	N	1	2
15min	6	596.3833	
30min	6		782.0500
60min	6		821.8167
Sig.		1.000	.084

Means for groups in homogeneous subsets are displayed.

a. Uses Harmonic Mean Sample Size = 6.000.

Table 13. Oneway ANOVA for ΔS values of 15-minute removal group in the second experiment

	Sum of Squares	df	Mean Square	F	Sig.
Between Groups	160076.988	2	80038.494	26.641	.000
Within Groups	45065.355	15	3004.357		
Total	205142.343	17			

Table 14. Duncan's multiple range test

Duncan[a]

		Subset for alpha = .05		
resin	N	1	2	3
Snap	6	596.3833		
Vertex	6		669.1667	
Duralay	6			822.6333
Sig.		1.000	1.000	1.000

Means for groups in homogeneous subsets are displayed.

a. Uses Harmonic Mean Sample Size = 6.000.

Table 15. Oneway ANOVA for ΔS values of 30-minute removal group in the second experiment

	Sum of Squares	df	Mean Square	F	Sig.
Between Groups	168635.444	2	84317.722	37.216	.000
Within Groups	33984.218	15	2265.615		
Total	202619.663	17			

Table 16. Duncan's multiple range test

Duncan[a]

resin	N	Subset for alpha = .05		
		1	2	3
Snap	6	782.0500		
Vertex	6		865.0500	
Duralay	6			1015.8833
Sig.		1.000	1.000	1.000

Means for groups in homogeneous subsets are displayed.

a. Uses Harmonic Mean Sample Size = 6.000.

Table 17. Oneway ANOVA for ΔS values of 60-minute removal group in the second experiment

	Sum of Squares	df	Mean Square	F	Sig.
Between Groups	378157.391	2	189078.696	42.999	.000
Within Groups	65958.512	15	4397.234		
Total	444115.903	17			

Table 18. Duncan's multiple range test

Duncan[a]

resin	N	Subset for alpha = .05		
		1	2	3
Snap	6	821.8167		
Vertex	6		959.8500	
Duralay	6			1174.1167
Sig.		1.000	1.000	1.000

Means for groups in homogeneous subsets are displayed.

a. Uses Harmonic Mean Sample Size = 6.000.

Table 19. Oneway ANOVA for shrinkage strains of 15-minute removal group at 180 minutes (S_{180}) in the second experiment

	Sum of Squares	df	Mean Square	F	Sig.
Between Groups	12803940	2	6401969.9	916.199	.000
Within Groups	104812.927	15	6987.528		
Total	12908753	17			

Table 20. Duncan's multiple range test

Duncan[a]

Resin	N	Subset for alpha = .05		
		1	2	3
Vertex	6	-2995.17		
Duralay	6		-2707.50	
Snap	6			-1079.63
Sig.		1.000	1.000	1.000

Means for groups in homogeneous subsets are displayed.

a. Uses Harmonic Mean Sample Size = 6.000.

Table 21. Oneway ANOVA for shrinkage strains of 30-minute removal group at 180 minutes (S_{180}) in the second experiment

	Sum of Squares	df	Mean Square	F	Sig.
Between Groups	7865146.6	2	3932573.3	904.082	.000
Within Groups	65246.948	15	4349.797		
Total	7930393.6	17			

Table 22. Duncan's multiple range test

Duncan[a]

		Subset for alpha = .05		
Resin	N	1	2	3
Vertex	6	-2650.32		
Duralay	6		-2434.30	
Snap	6			-1152.60
Sig.		1.000	1.000	1.000

Means for groups in homogeneous subsets are displayed.

a. Uses Harmonic Mean Sample Size = 6.000.

Table 23. Oneway ANOVA for shrinkage strains of 60-minute removal group at 180 minutes (S_{180}) in the second experiment

	Sum of Squares	df	Mean Square	F	Sig.
Between Groups	7227621.7	2	3613810.9	584.670	.000
Within Groups	92714.072	15	6180.938		
Total	7320335.8	17			

Table 24. Duncan's multiple range test

Duncan[a]

		Subset for alpha = .05		
Resin	N	1	2	3
Vertex	6	-2856.88		
Duralay	6		-2454.18	
Snap	6			-1357.35
Sig.		1.000	1.000	1.000

Means for groups in homogeneous subsets are displayed.

a. Uses Harmonic Mean Sample Size = 6.000.

Table 25. Oneway ANOVA for linear thermal expansion coefficient of 15-minute heat-soaking regime in the third experiment

	Sum of Squares	df	Mean Square	F	Sig.
Between Groups	2614.266	2	1307.133	10.961	.002
Within Groups	1431.053	12	119.254		
Total	4045.319	14			

Table 26. Duncan's multiple range test

Duncan[a]

Resin	N	Subset for alpha = .01	
		1	2
Snap	5	49.5620	
Vertex	5		70.9600
Duralay	5		81.2580
Sig.		1.000	.162

Means for groups in homogeneous subsets are displayed.

a. Uses Harmonic Mean Sample Size = 5.000.

Table 27. Oneway ANOVA for linear thermal expansion coefficient of 45-minute heat-soaking regime in the third experiment

	Sum of Squares	df	Mean Square	F	Sig.
Between Groups	3312.023	2	1656.011	45.792	.000
Within Groups	433.967	12	36.164		
Total	3745.990	14			

Table 28. Duncan's multiple range test

Duncan[a]

Resin	N	Subset for alpha = .01		
		1	2	3
Snap	5	48.6700		
Vertex	5		69.6340	
Duralay	5			84.9200
Sig.		1.000	1.000	1.000

Means for groups in homogeneous subsets are displayed.

a. Uses Harmonic Mean Sample Size = 5.000.

Table 29. Oneway ANOVA for shrinkage strain at 180 minutes for 15-minute heat-soaking regime in the third experiment

S180

	Sum of Squares	df	Mean Square	F	Sig.
Between Groups	5369374.0	2	2684687.0	361.115	.000
Within Groups	89213.204	12	7434.434		
Total	5458587.2	14			

Table 30. Duncan's multiple range test

Duncan[a]

resin	N	Subset for alpha = .01		
		1	2	3
Vertex	5	-2416.68		
Duralay	5		-2045.08	
Snap	5			-1003.18
Sig.		1.000	1.000	1.000

Means for groups in homogeneous subsets are displayed.

a. Uses Harmonic Mean Sample Size = 5.000.

Table 31. Oneway ANOVA for shrinkage strain at 180 minutes for 45-minute heat-soaking regime in the third experiment

S180

	Sum of Squares	df	Mean Square	F	Sig.
Between Groups	13258722	2	6629361.1	736.998	.000
Within Groups	107941.028	12	8995.086		
Total	13366663	14			

Table 32. Duncan's multiple range test

Duncan[a]

		Subset for alpha = .01		
resin	N	1	2	3
Vertex	5	-2694.38		
Duralay	5		-2278.46	
Snap	5			-524.8200
Sig.		1.000	1.000	1.000

Means for groups in homogeneous subsets are displayed.

a. Uses Harmonic Mean Sample Size = 5.000.